Possible cubic Dirac point and quadratic Weyl point in ε-TaN

Peng-Jen Chen (陳鵬仁)

Institute of Physics, Academia Sinica

Institute of Atomic and Molecular Sciences, Academia Sinica (beginning from 7/1/2019)

06/25/2019 at the 17th Workshop on First-Principles Computational Materials

Outline

- feature of electronic structure in materials with space group 194
- order of Dirac point and Weyl points with high chiral charge
  - Computational results
  - discussions

Structure and symmetries in materials with space 194

ε-TaN

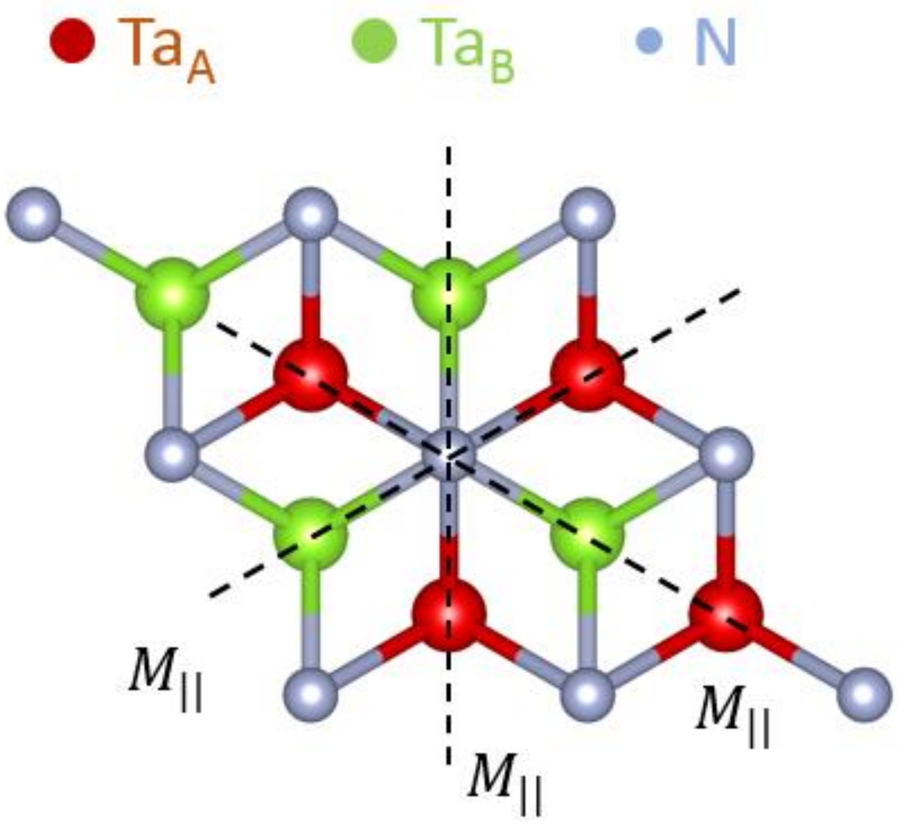

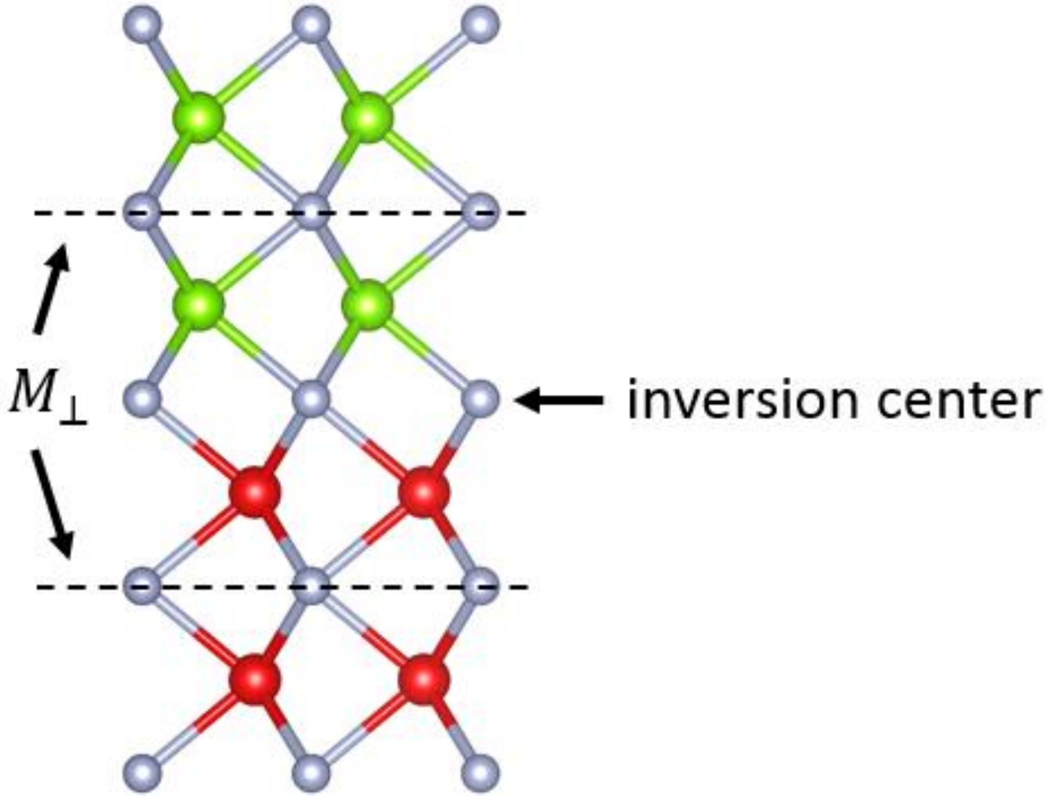

- inversion
- mirror symmetry
  - three $M_{||}$ and two $M_{\perp}$
- C_3 rotation symmetry
- S_6 screw symmetry
  (rotation + half translation along the rotation axis)

Band dispersion around $k_z = \pi/c$ in materials with space group 194

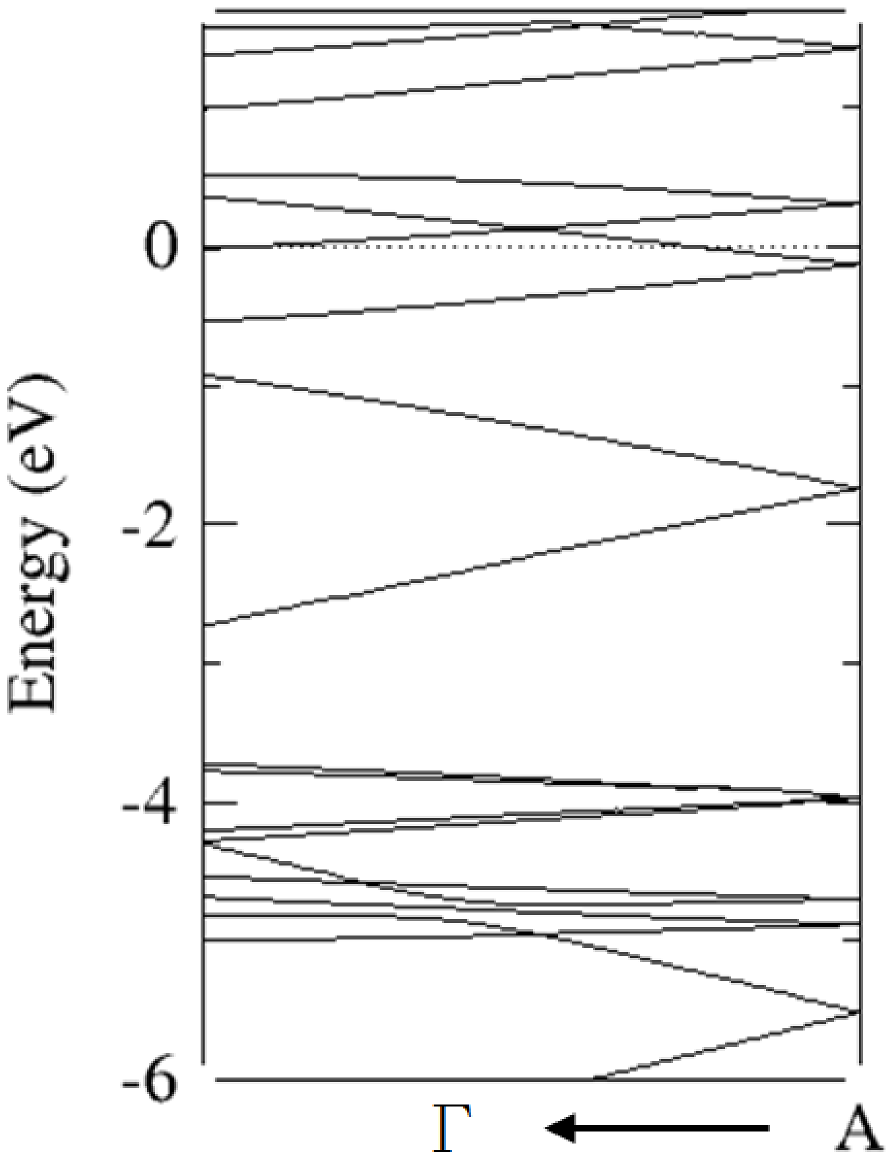

- The two sublattices are symmetric under the screw operation.
- The states on the rotation axis do not sense the difference due to the rotation; each sublattice acts as if it is a duplicate of the other.
- The bands are "folded back" when they hit the zone boundary ($k_z = \pi/c$).
- A DP can happen when two such "band foldings" are close in energy.

Electronic and topological properties of ε-TaN

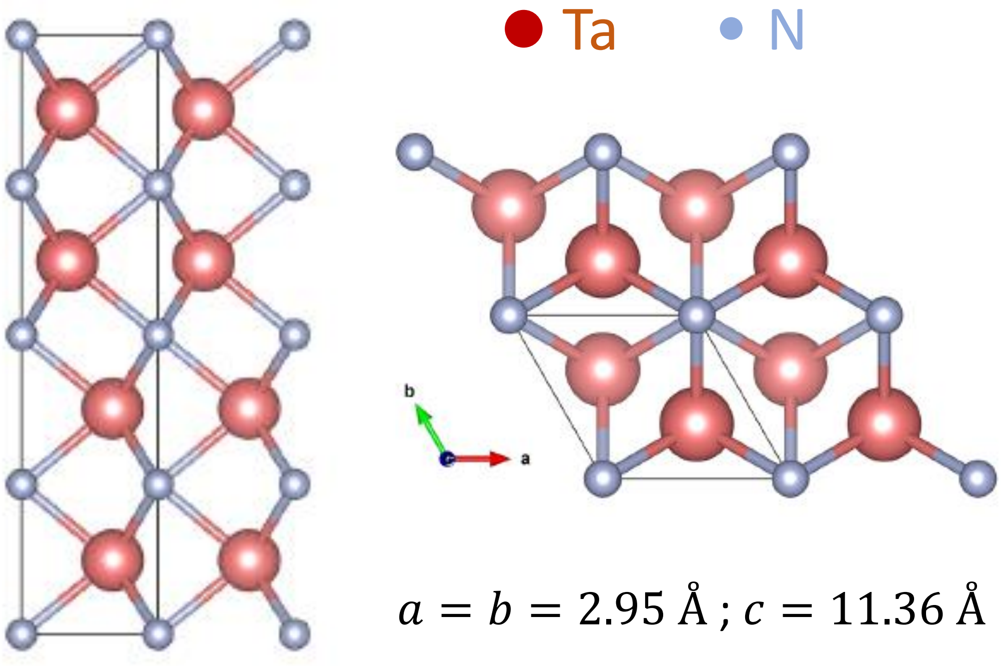

$a = b = 2.95$ Å ; $c = 11.36$ Å

TABLE I. The parities at the TRIM of ε-TaN. It is apparent that the 2D plane with $k_z = 0$ (containing Γ and M points) reveals nontrivial Z_2. The $k_z = \pi/c$ plane, on the other hand, is Z_2-trivial.

Γ	3M	A	3L
−	+	+	+

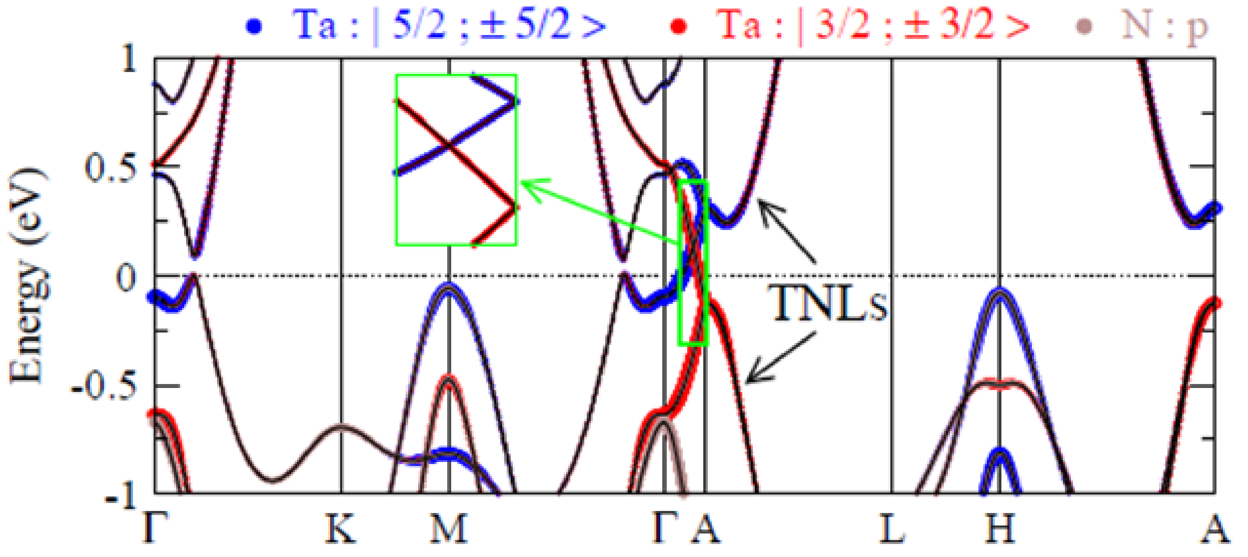

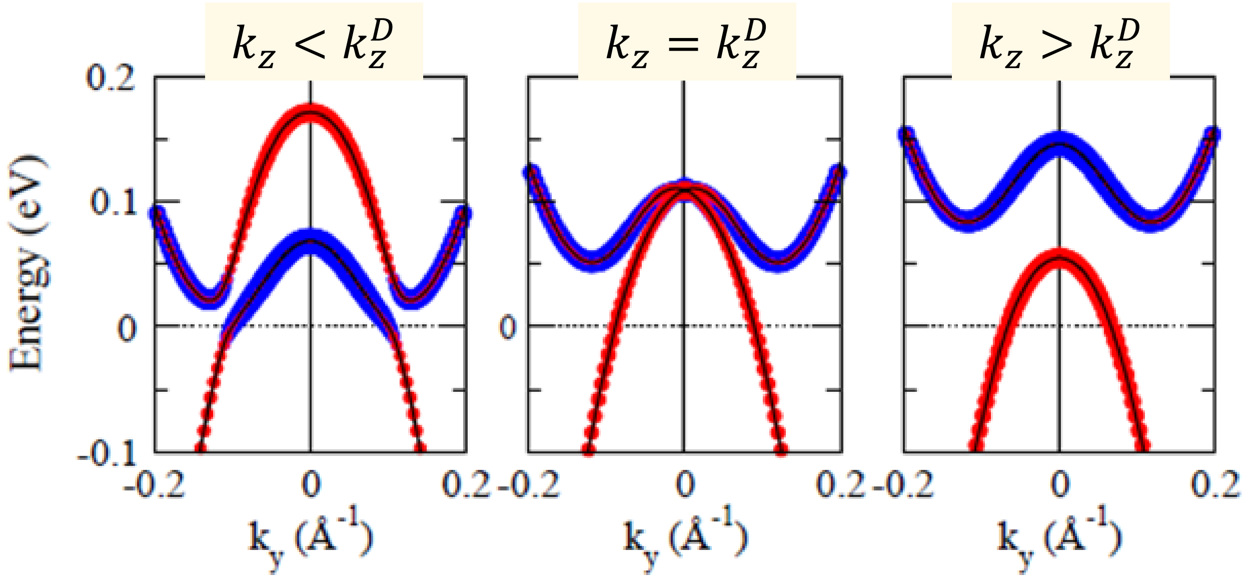

Dirac semimetals

- Dirac point (DP): crossing of two doubly degenerate bands
- Mostly, the Dirac bands show linear dispersion.

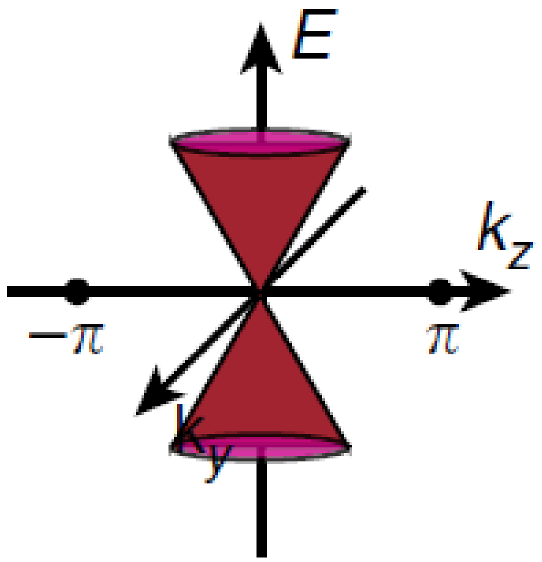

Na_3Bi

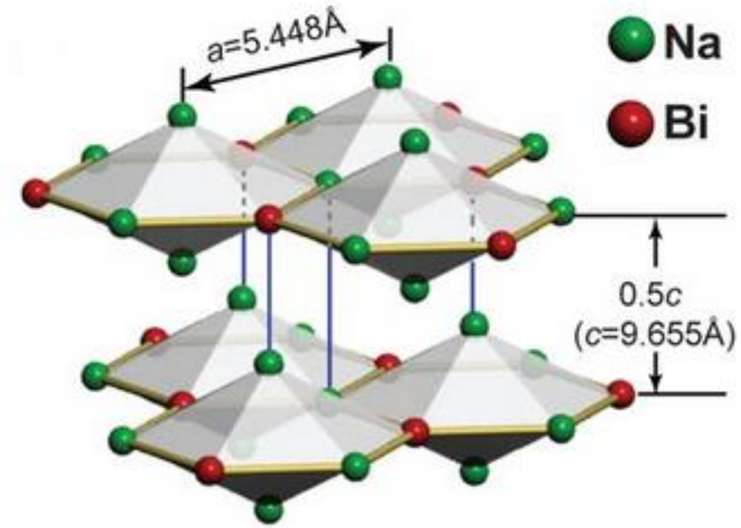

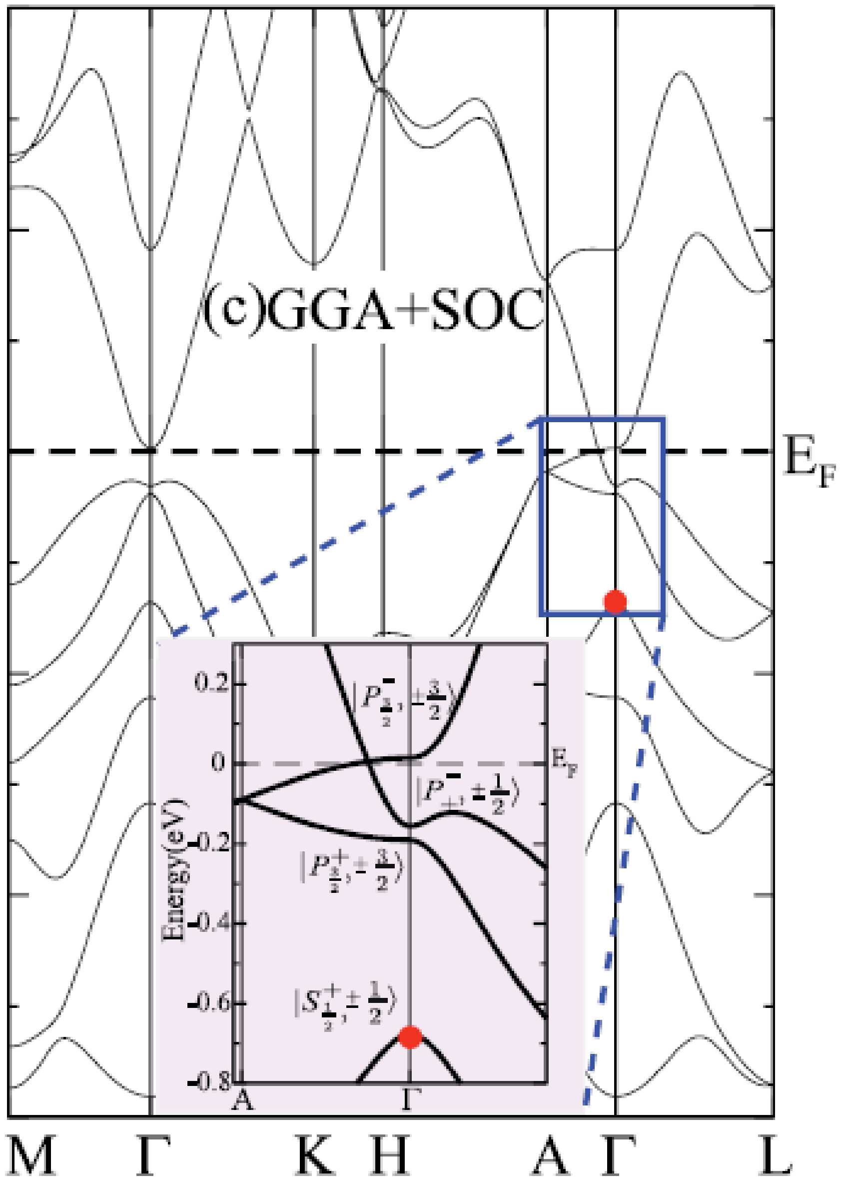

Order of Dirac point

in-plane dispersion

linear DP

$$H_{\text{Dirac}}(\mathbf{q}) \sim \begin{pmatrix} q_x\tau_x + q_y\tau_y + q_z\tau_z & 0 \\ 0 & -q_x\tau_x - q_y\tau_y - q_z\tau_z \end{pmatrix}$$

$$E \propto |q_{||}|$$

quadratic DP

$$H_{\text{Dirac}}(\mathbf{q}) \sim \begin{pmatrix} (q_x^2 - q_y^2)\tau_x + 2q_xq_y\tau_y + q_z\tau_z & 0 \\ 0 & -(q_x^2 - q_y^2)\tau_x - 2q_xq_y\tau_y - q_z\tau_z \end{pmatrix}$$

$$E \propto |q_{||}|^2$$

cubic DP

$$H_{\text{Dirac}}(\mathbf{q}) \sim \begin{pmatrix} (q_+^3 + q_-^3)\tau_x + i(q_+^3 - q_-^3)\tau_y + q_z\tau_z & 0 \\ 0 & -(q_+^3 + q_-^3)\tau_x - i(q_+^3 - q_-^3)\tau_y - q_z\tau_z \end{pmatrix}$$

$$E \propto |q_{||}|^3$$

Order of Dirac point versus rotation symmetry

ARTICLE

Received 24 Mar 2014 | Accepted 1 Aug 2014 | Published 15 Sep 2014

DOI: 10.1038/ncomms5898

Classification of stable three-dimensional Dirac semimetals with nontrivial topology

Bohm-Jung Yang[1] & Naoto Nagaosa[1,2]

$$H(\mathbf{k}) = \sum_{i,j=0}^{3} a_{ij}(\mathbf{k})\sigma_i\tau_j = \begin{pmatrix} h_{\uparrow\uparrow}(\mathbf{k}) & h_{\uparrow\downarrow}(\mathbf{k}) \\ h_{\downarrow\uparrow}(\mathbf{k}) & h_{\downarrow\downarrow}(\mathbf{k}) \end{pmatrix}$$

$$h_{\uparrow\uparrow}(\mathbf{k}) = f(\mathbf{k})\tau_+ + f^*(\mathbf{k})\tau_- + a_5(\mathbf{k})\tau_z$$

$$h_{\uparrow\downarrow}(\mathbf{k}) = g(\mathbf{k})\tau_x \text{ when } P = \pm\tau_z$$

$$h_{\uparrow\downarrow}(\mathbf{k}) = g(\mathbf{k})\tau_y \text{ when } P = \pm\tau_0$$

Table 1 | Classification table for 3D topological Dirac semimetals.

C_n	$\|P\|$	$(u_{A,\uparrow}, u_{B,\uparrow})$	$f(k_\pm, k_z)$	$g(k_\pm, k_z)$	2D topological invariant	$H_{Dirac}(q)$	Materials
C_2	τ_z	—	—	—	—	Not allowed	
C_2	τ_0	—	—	—	—	Not allowed	
C_3	τ_z	$(e^{i\pi}, e^{i\frac{\pi}{3}})$	βk_+	γk_-	$\nu_{2D} = 1$	Linear Dirac	Na_3Bi[17]
C_3	τ_0	$(e^{i\pi}, e^{i\frac{\pi}{3}})$	$\beta k_z k_+ + \gamma k_-^2$	$\eta k_z k_- + \xi k_+^2$	$\nu_{2D} = 0$	Linear Dirac	
C_4	τ_z	$(e^{i\frac{3\pi}{4}}, e^{i\frac{\pi}{4}})$	ηk_+	$\beta k_z k_+^2 + \gamma k_z k_-^2$	$n_M = \pm 1$	Linear Dirac	Cd_3As_2[18]
C_4	τ_0	$(e^{i\frac{3\pi}{4}}, e^{i\frac{\pi}{4}})$	$\eta k_z k_+$	$\beta k_+^2 + \gamma k_-^2$	$n_M = 2\mathrm{sgn}(\|\beta\| - \|\gamma\|)$	Linear Dirac	
C_6	τ_z	$(e^{i\frac{\pi}{2}}, e^{i\frac{\pi}{6}})$	βk_+	$\gamma k_z k_+^2$	$n_M = \pm 1$	Linear Dirac	
C_6	τ_0	$(e^{i\frac{\pi}{2}}, e^{i\frac{\pi}{6}})$	$\beta k_z k_+$	γk_+^2	$n_M = \pm 2$	Linear Dirac	
C_6	τ_z	$(e^{i\frac{5\pi}{6}}, e^{i\frac{\pi}{2}})$	βk_+	$\gamma k_z k_-^2$	$n_M = \pm 1$	Linear Dirac	
C_6	τ_0	$(e^{i\frac{5\pi}{6}}, e^{i\frac{\pi}{2}})$	$\beta k_z k_+$	γk_-^2	$n_M = \pm 2$	Linear Dirac	
C_6	τ_z	$(e^{i\frac{5\pi}{6}}, e^{i\frac{\pi}{6}})$	$\eta k_z k_+^2$	$\beta k_+^3 + \gamma k_-^3$	$n_M = 3\mathrm{sgn}(\|\beta\| - \|\gamma\|)$	Quadratic Dirac	
C_6	τ_0	$(e^{i\frac{5\pi}{6}}, e^{i\frac{\pi}{6}})$	ηk_+^2	$\beta k_z k_+^3 + \gamma k_z k_-^3$	$n_M = \pm 2$	Quadratic Dirac	

Dispersion of the Dirac bands

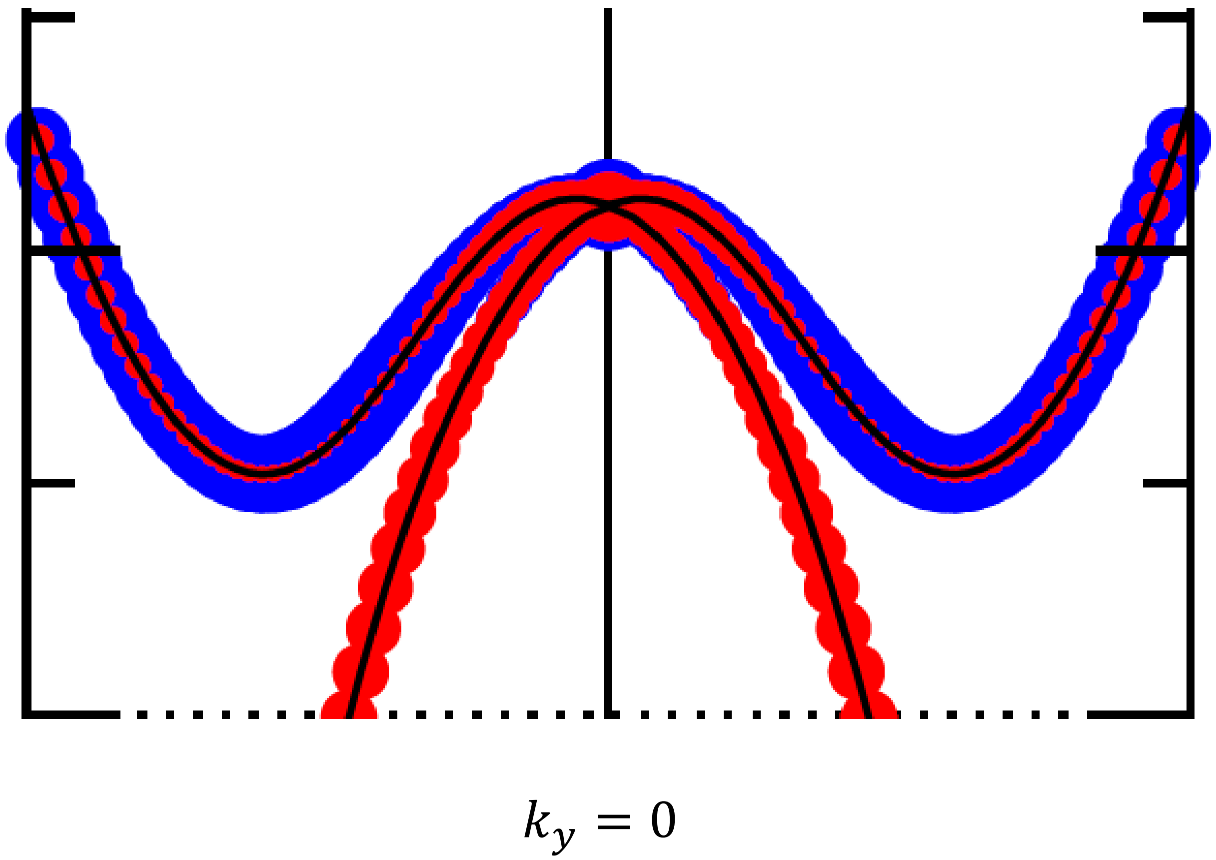

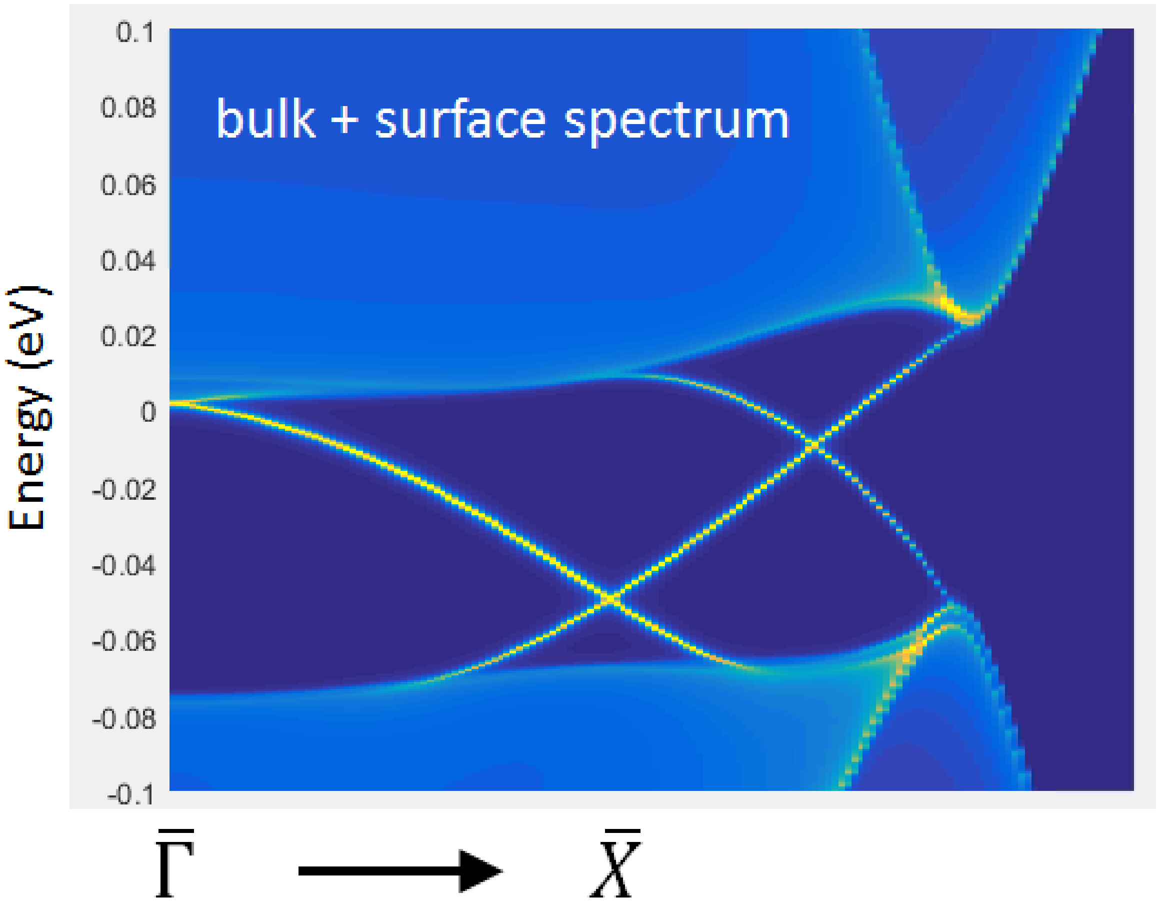

linear DP: $E \propto |q_{||}|$

quadratic DP: $E \propto |q_{||}|^2$

cubic DP: $E \propto |q_{||}|^3$

Application of an out-of-plane Zeeman field

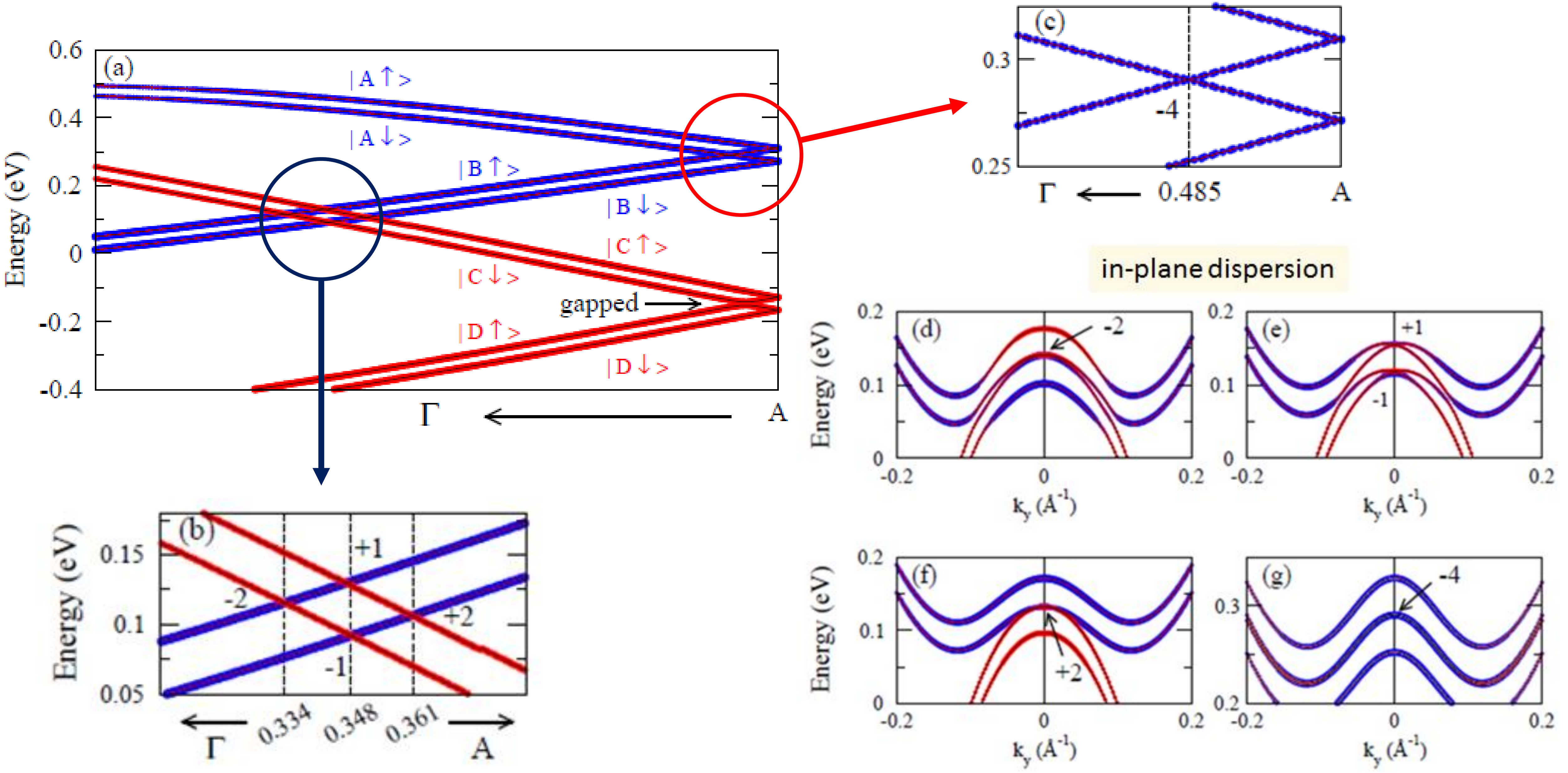

Methods to compute the chiral charge of a Weyl point

1. Wilson loop

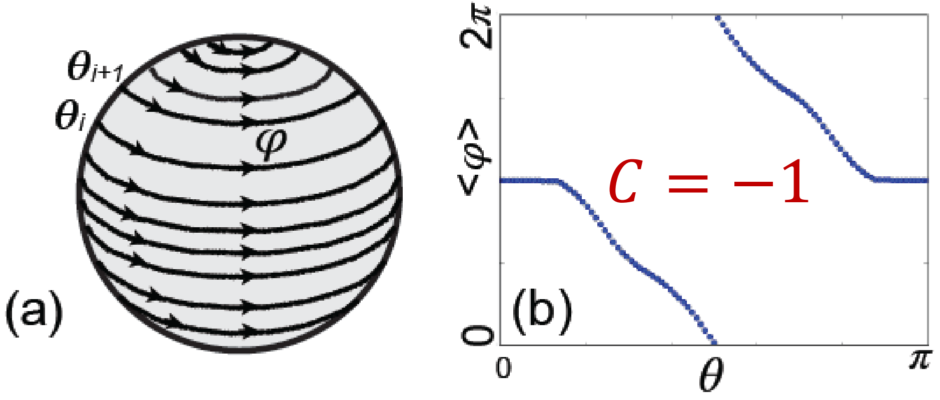

Nature **527**, 495-498

(Supplementary Information)

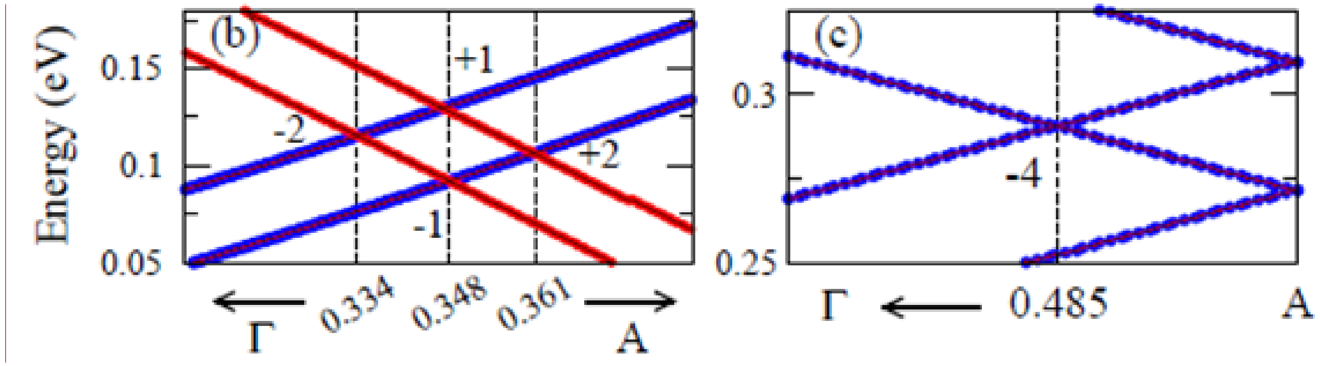

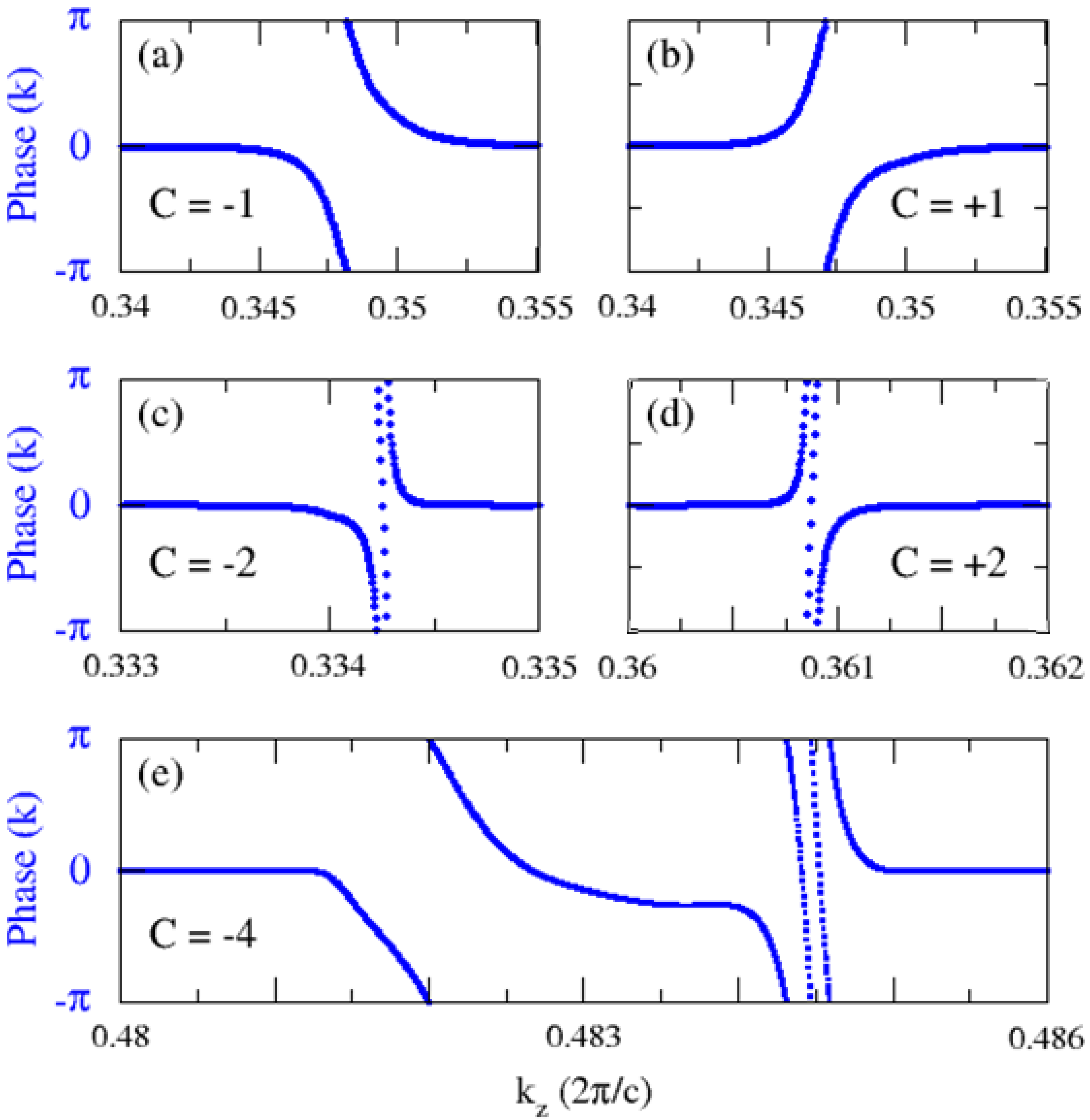

Methods to compute the chiral charge of a Weyl point

2. change in Chern number

$$C(k_z) = \frac{1}{2\pi}\int_{BZ} \Omega(k_z) d^2k$$

It requires that the effective 2D system (fixed k_z) be gapped.

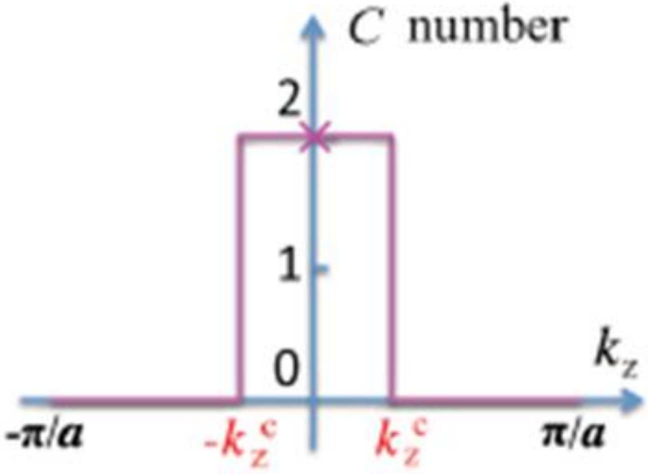

PRL **107**, 186806 (2011)

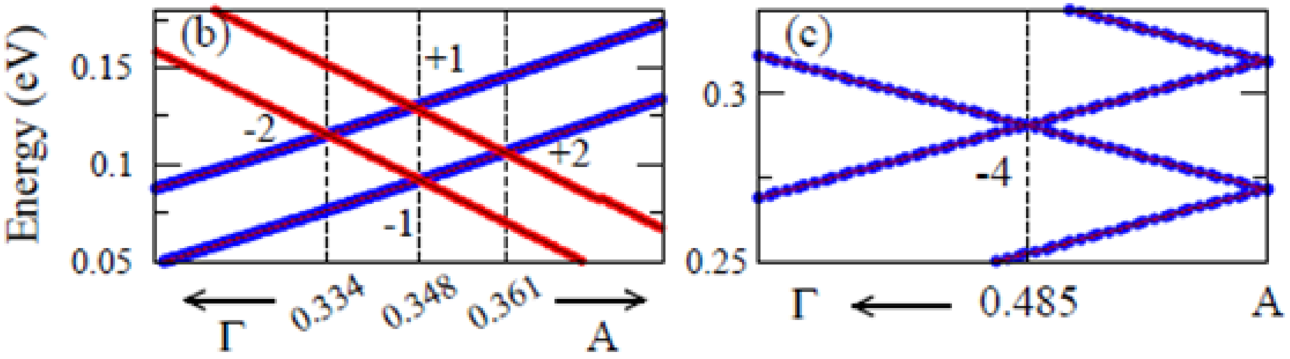

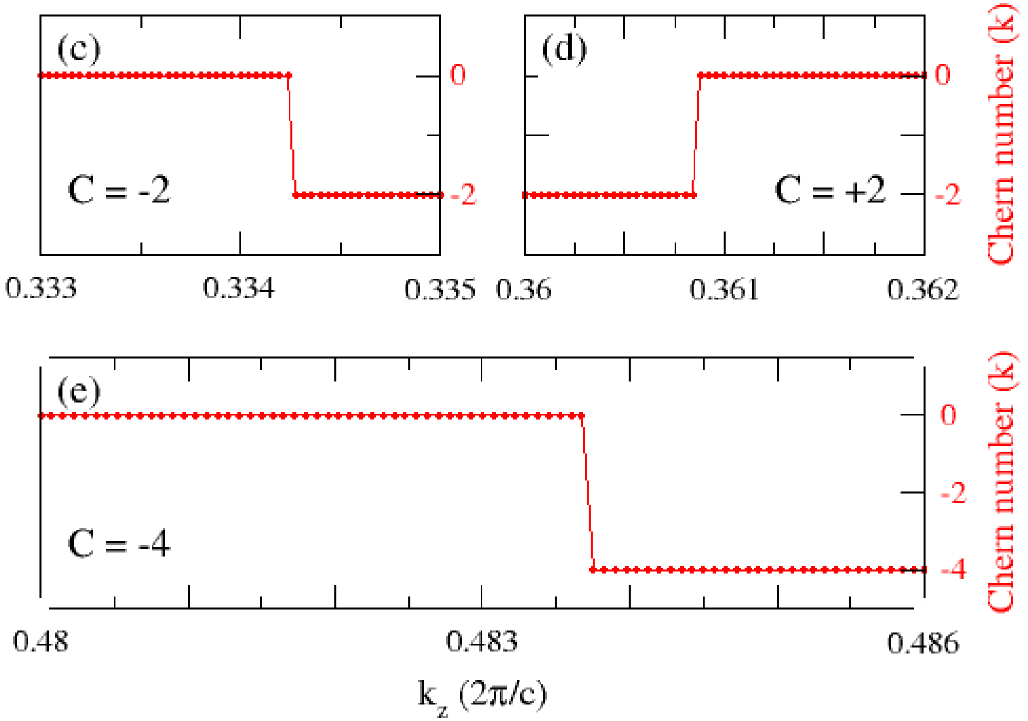

Methods to compute the chiral charge of a Weyl point

3. Ratio of the rotation (screw) eigenvalues of conduction and valence bands (u_c/u_v)

For C_m invariant systems

chiral charge

m	u_c/u_v	$\approx$	Q
2	-1		$\mathrm{sgn}(\lvert a\rvert - \lvert b\rvert)$
3	$e^{\pm i2\pi/3}$		± 1
4	$\pm i$		± 1
	-1		$2\mathrm{sgn}(\lvert a\rvert - \lvert b\rvert)$
6	$e^{\pm i\pi/3}$		± 1
	$e^{\pm i2\pi/3}$		± 2
	-1		$3\mathrm{sgn}(\lvert a\rvert - \lvert b\rvert)$

PRL **108**, 266802 (2012)

This method applies when the Weyl points are located at the rotation (screw)-invariant momenta (e.g. on the rotation axis).

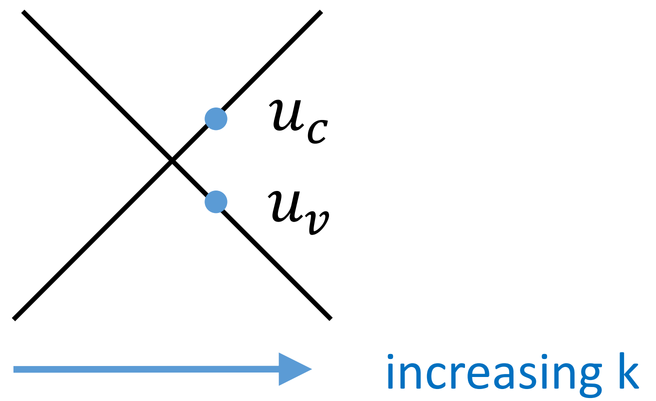

Since m cannot exceed six in a real material, there seems to be an upper limit of chiral charge ($C \leq 3$).

Upper limit for chiral charge?

$$H_{\text{eff}}(\mathbf{K}+\mathbf{q}) = f(\mathbf{q})\sigma_+ + f^*(\mathbf{q})\sigma_- + g(\mathbf{q})\sigma_z$$

m	u_c/u_v	Constraints on f	H_{eff}	Q
6	$e^{\pm i\pi/3}$	$f(q_+e^{i\pi/3}, q_-e^{i\pi/3}) = e^{\pm i\pi/3} f(q_+, q_-)$	$m\sigma_z + aq_+\sigma_+ + \text{H.c.}$	± 1
	$e^{\pm i2\pi/3}$	$f(q_+e^{i\pi/3}, q_-e^{i\pi/3}) = e^{\pm i2\pi/3} f(q_+, q_-)$	$m\sigma_z + aq_\pm^2\sigma_+ + \text{H.c.}$	± 2
	-1	$f(q_+e^{i\pi/3}, q_-e^{i\pi/3}) = -f(q_+, q_-)$	$m\sigma_z + (aq_+^3 + bq_-^3)\sigma_+ + \text{H.c.}$	$3\text{sgn}(\lvert a\rvert - \lvert b\rvert)$

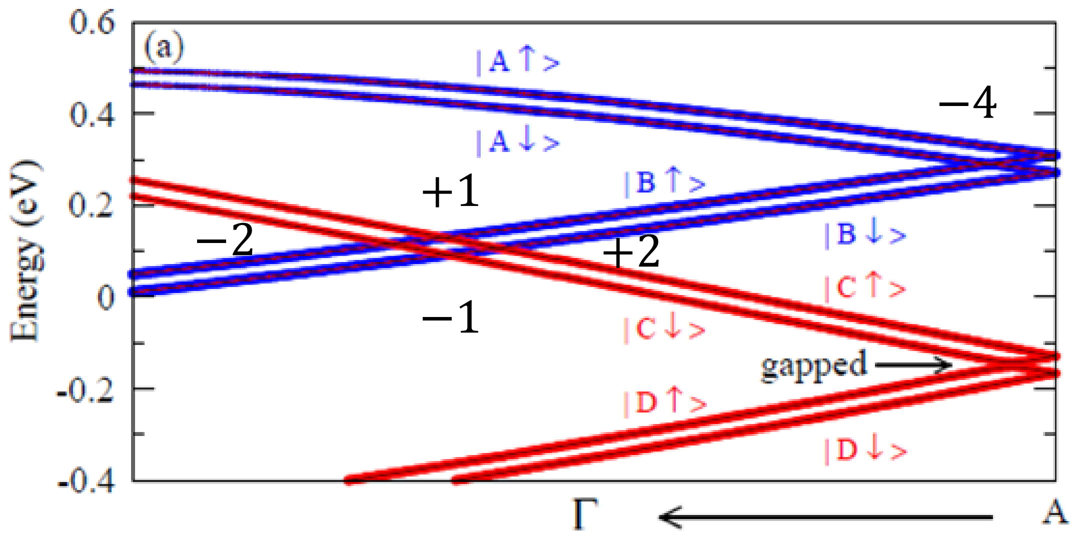

TABLE II. The calculated phases (θ), in unit of $\frac{n\pi}{3}$, of the screw eigenvalues ($\lambda = e^{i\theta}$) of the eight bands labeled in Fig. 3(a). Difference in n between two crossed bands indicates the chiral charge of the WP.

band	$\lvert A\uparrow\rangle$	$\lvert A\downarrow\rangle$	$\lvert B\uparrow\rangle$	$\lvert B\downarrow\rangle$	$\lvert C\uparrow\rangle$	$\lvert C\downarrow\rangle$	$\lvert D\uparrow\rangle$	$\lvert D\downarrow\rangle$
n	-2	5	1	2	0	3	3	0
λ	$e^{-i\frac{2\pi}{3}}$	$e^{i\frac{5\pi}{3}}$	$e^{i\frac{\pi}{3}}$	$e^{i\frac{2\pi}{3}}$	1	-1	-1	1

Upper limit for chiral charge?

$$\frac{u_c}{u_v} = \frac{e^{i\theta_1}}{e^{i\theta_2}} = e^{i2\pi C/m}$$

$$\Delta\theta = \theta_1 - \theta_2 \not\equiv 2\pi C/m$$

$$e^{iA} = e^{iB} \rightarrow A = B \pm 2n\pi$$

- The value of C so obtained is simply the chiral charge mod m.
- There (in principle) should not be an upper limit for the chiral charge.

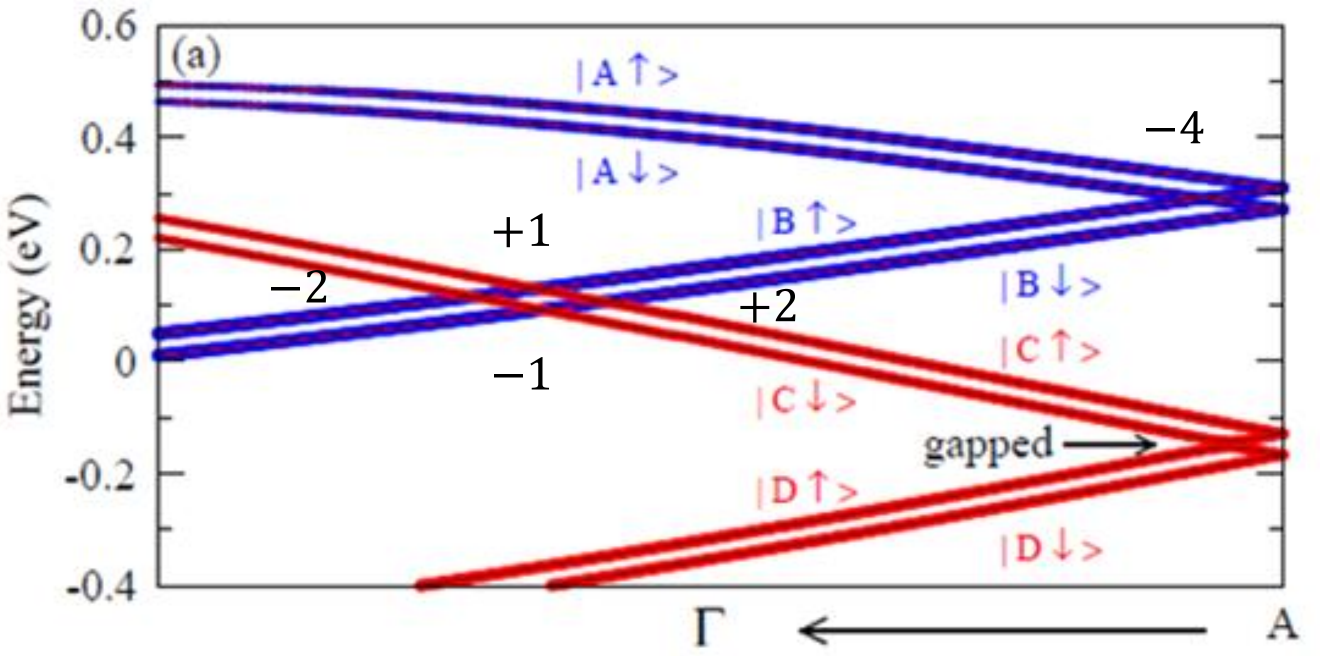

TABLE II. The calculated phases (θ), in unit of $\frac{n\pi}{3}$, of the screw eigenvalues ($\lambda = e^{i\theta}$) of the eight bands labeled in Fig. 3(a). Difference in n between two crossed bands indicates the chiral charge of the WP.

band	$\lvert A\uparrow\rangle$	$\lvert A\downarrow\rangle$	$\lvert B\uparrow\rangle$	$\lvert B\downarrow\rangle$	$\lvert C\uparrow\rangle$	$\lvert C\downarrow\rangle$	$\lvert D\uparrow\rangle$	$\lvert D\downarrow\rangle$
n	-2	5	1	2	0	3	3	0
λ	$e^{-i\frac{2\pi}{3}}$	$e^{i\frac{5\pi}{3}}$	$e^{i\frac{\pi}{3}}$	$e^{i\frac{2\pi}{3}}$	1	-1	-1	1

Constraint from the topological nodal-lines

Candidate system	Space group	Relevant symmetry	Shape of line nodes	Number of line nodes
$\hat{H}^{(0)}$	59	$\widetilde{M}_x^{\perp}$ or $\widetilde{M}_y^{\perp}$	open straight	2
$\hat{H}^{(0)} + \delta H^{(1)}(k)$	11	$\widetilde{M}_x^{\perp}$	open	1
BaTaS	194	$\widetilde{M}_z^{\perp}$	open straight	3
$SrIrO_3$	62	$\widetilde{C}_{2z}^{\parallel,\perp}$ and $\widetilde{C}_{2y}^{\parallel}$	closed loop	1

PHYSICAL REVIEW B **95**, 075135 (2017)

The off-centered glide symmetry protects the topological nodal-lines (TNLs) at $k_z = \pi/c$ plane for materials with space group 194.

- The winding number (Berry phase) of each TNL is 1 (2π).
- Viewing the crossing point A as an effective "topological point", we speculate that the phase change would be π (each TNL contributes $\pi/3$)

$BaTaS_3$

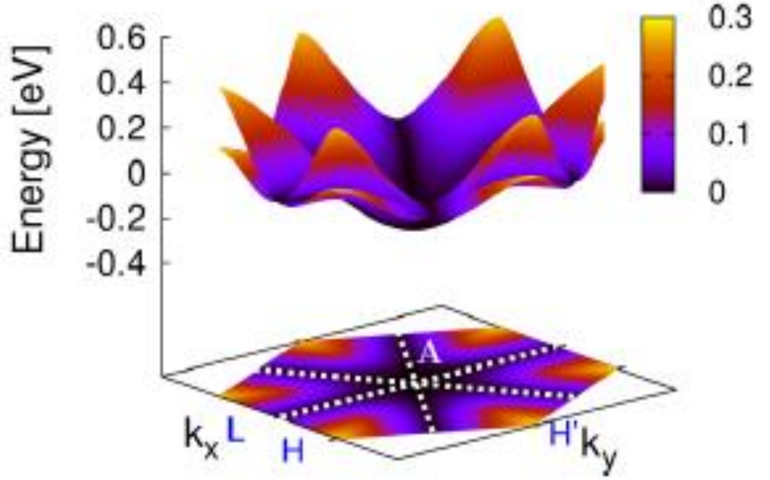

PHYSICAL REVIEW B **93**, 085427 (2016)

Phase difference when crossing *A* point

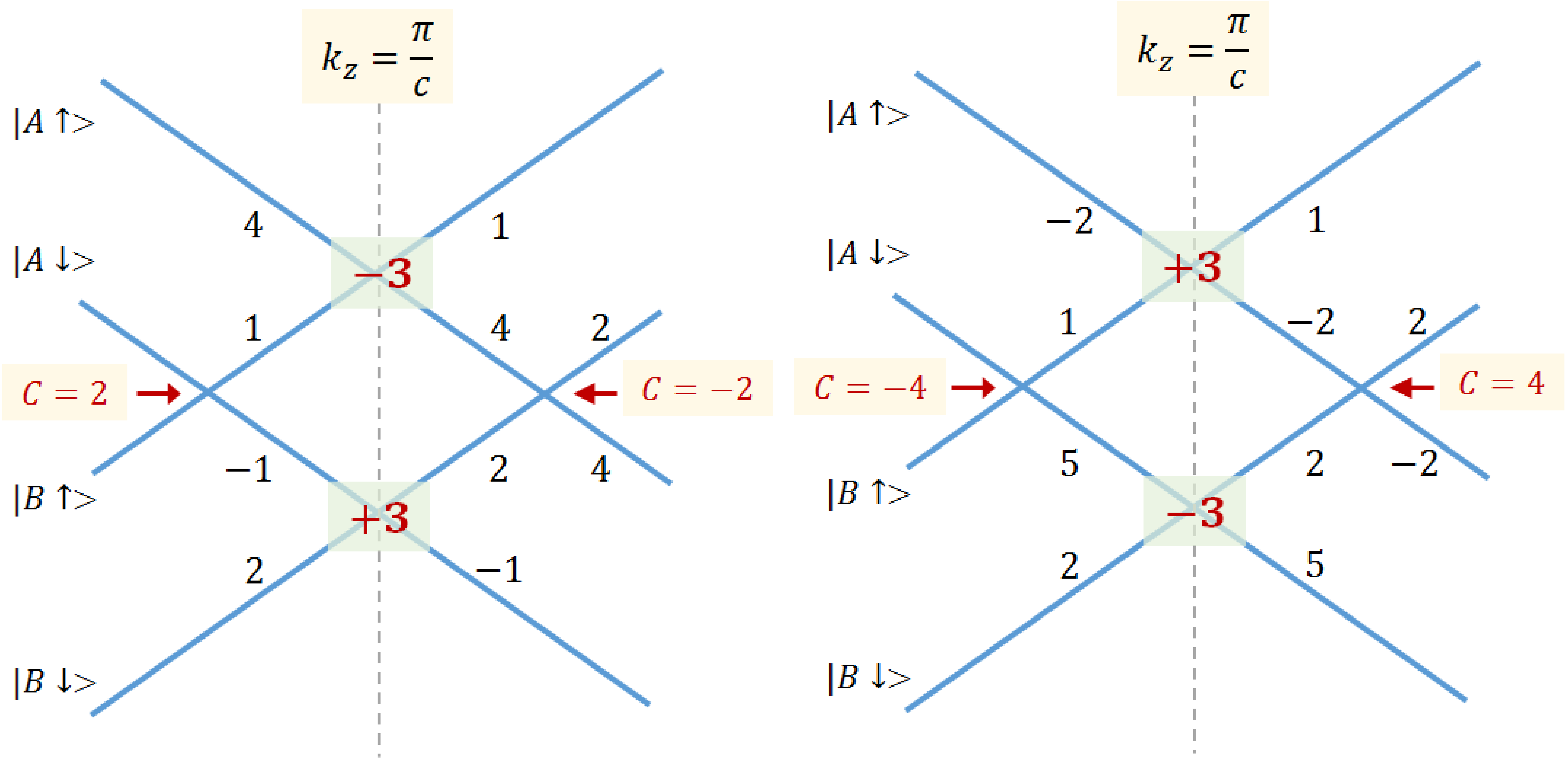

Comparison study: Na_3Bi

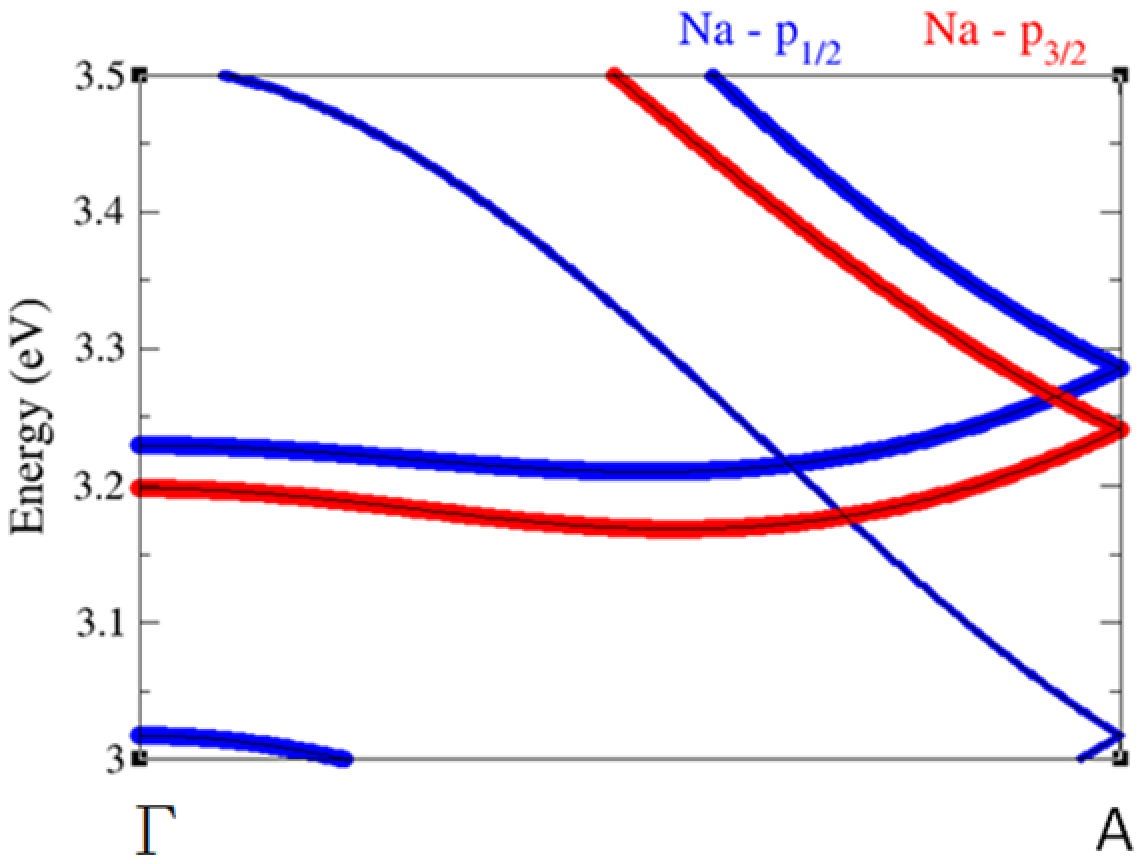

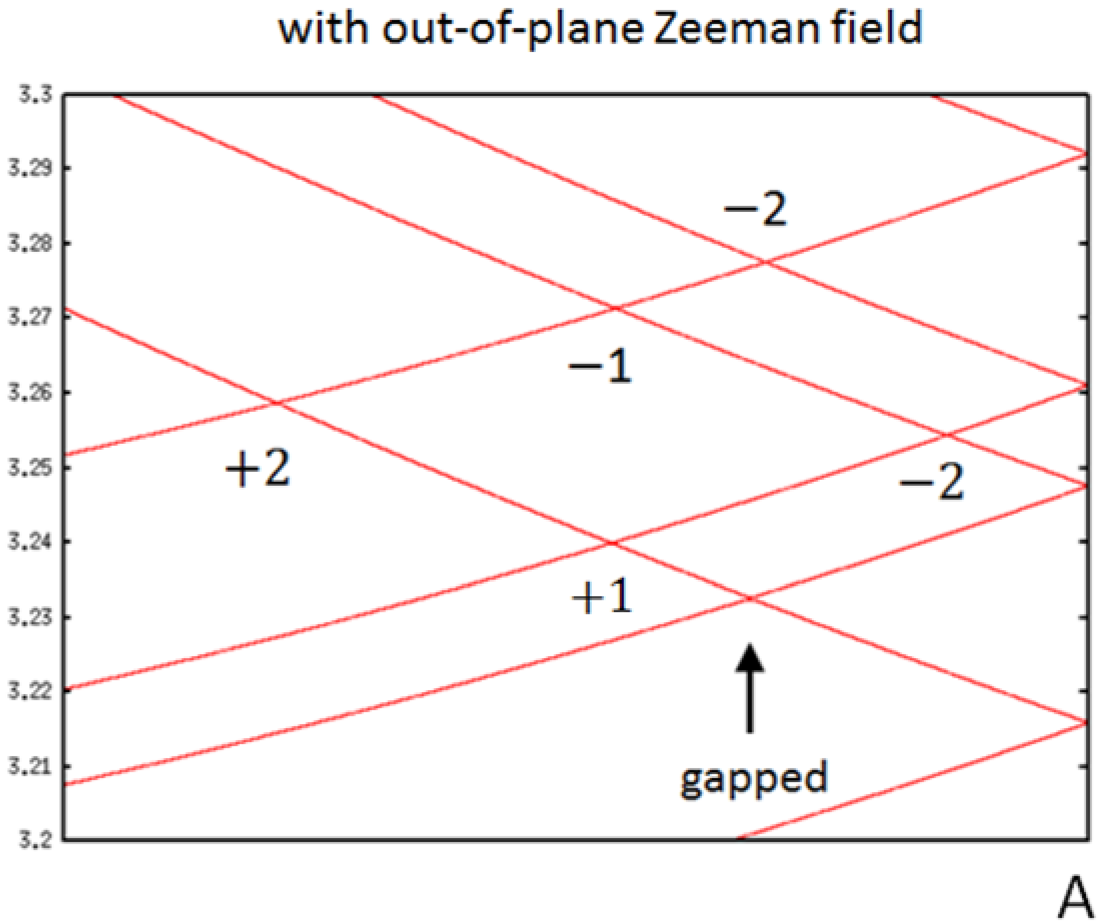

The symmetry representations in space group 194 cannot guarantee a Weyl point with $|C| = 4$.

Cubic Dirac point as a single point?

Classification of stable three-dimensional Dirac semimetals with nontrivial topology

Bohm-Jung Yang[1] & Naoto Nagaosa[1,2]

NATURE COMMUNICATIONS | 5:4898 | DOI: 10.1038/ncomms5898

Table 2 | Classification table for 3D Dirac SMs with a single Dirac point.

C_n	$\lvert P\rvert$	$u_{A,\uparrow}$	$f(k_\pm, k_z)$	$g_z(k_\pm, k_z)$	$H_{Dirac}(q)$	Material
C_2	τ_x	$e^{i\frac{\pi}{2}}$	$k_z F_1^{(1)}(k_{x,y}) - iF_2^{(1)}(k_{x,y})$	$\alpha k_x + \beta k_y$	Linear Dirac	Distorted spinels[16]
C_3	τ_x	—	—	—	Not allowed	
C_4	τ_x	$e^{\pm i\frac{\pi}{4}}$	$F_1^{(2)}(k_{x,y}) - ik_z F_2^{(2)}(k_{x,y})$	$\alpha k_\pm$	Linear Dirac	BiO_2[15]
C_6	τ_x	$e^{\pm i\frac{\pi}{6}}$	$k_z F_1^{(3)}(k_{x,y}) + iF_2^{(3)}(k_{x,y})$	$\alpha k_\pm$	Linear Dirac	
C_6	τ_x	$e^{i\frac{3\pi}{6}}$	$k_z F_1^{(3)}(k_{x,y}) + iF_2^{(3)}(k_{x,y})$	$F_3^{(3)}(k_{x,y}) + iF_4^{(3)}(k_{x,y})$	Cubic Dirac	

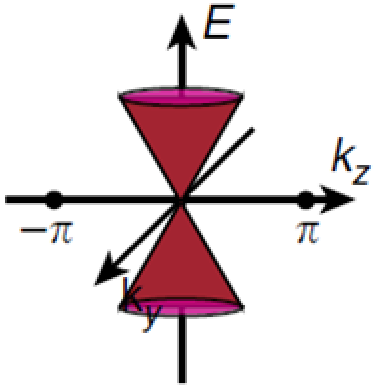

- A single Dirac point is located at time-reversal invariant momenta (TRIM).
- This is a consequence of a four-band model and is not universally true.

Four-band model for a Dirac point

parity: $P = \pm\tau_0$ or $\pm\tau_z$ (even)

$P = \pm\tau_x$ (odd)

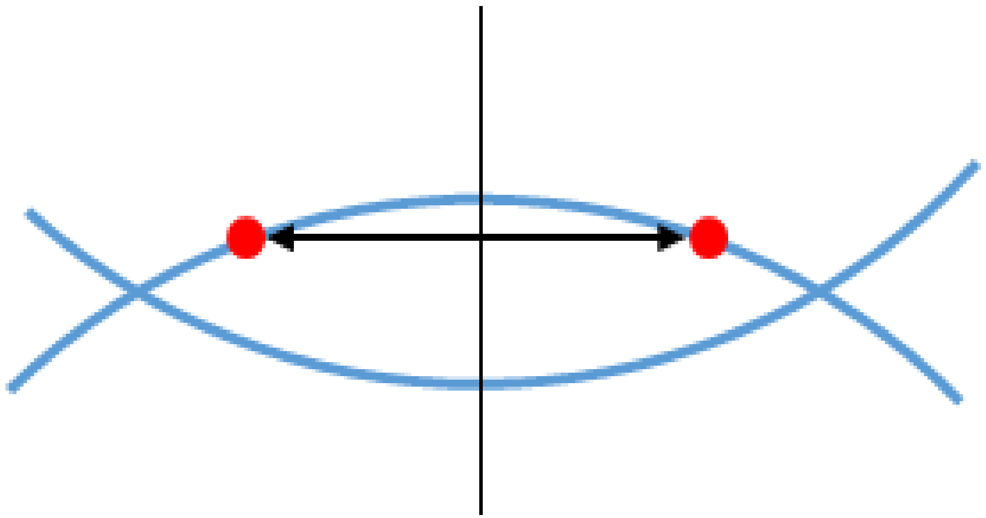

- The operation of P maps states belonging to the same band.
- a pair of DPs

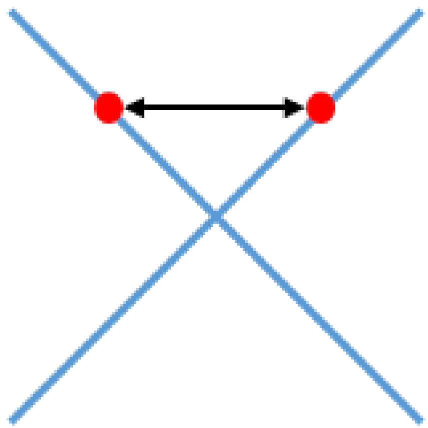

- The operation of P maps states belonging to different bands.
- single DP at the TRIM

Cubic Dirac point can be present only when $P = \pm\tau_x$ and must appear as a single point at the TRIM.

Eight-band model and beyond

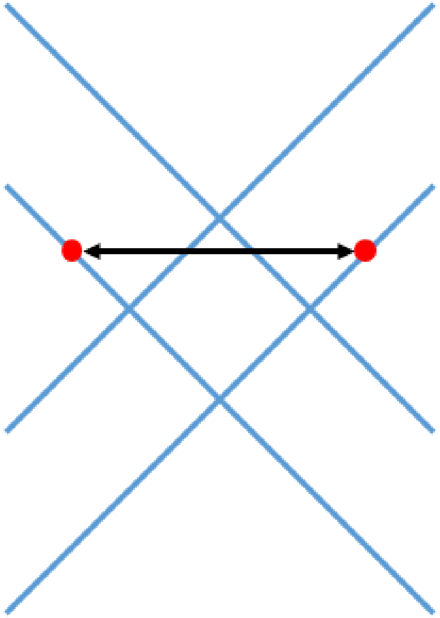

PHYSICAL REVIEW B 93, 085427 (2016)

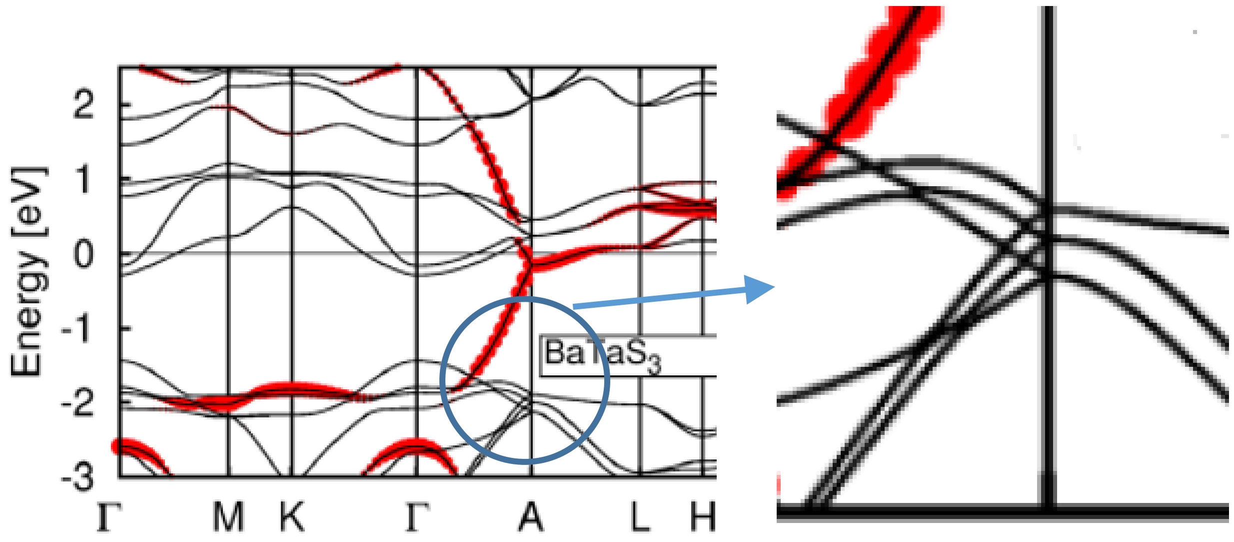

- In our case, the four-band model is not enough to describe the behaviors around the DP.
- In an eight-band model, $P = \pm\tau_x$ can hold for DPs away from the TRIM (but remaining on the rotation axis).

- Similar band crossings are also found in (SG-194 phase) $PbTaSe_2$.
- For binary (ternary) SG-194 materials, there exist DPs in a eight-band (twelve-band) manifold.

Summary

- In materials with space group 194:
  - the screw symmetry gives rise to "band folding" at $A\ (0, 0, \pi/c)$.
  - TNLs are present on $k_z = \pi/c$ plane and cross at A.
  - When two such "folded bands" are close in energy, a cubic Dirac point can take place.
- Under the application of out-of-plane Zeeman field, high-order Weyl points may appear due to accidental band crossing. The chiral charge of such Weyl point is connected to the chirality of the TNLs.
- In ε-TaN, as well as ε-NbN, high-order Weyl points ($C = \pm 4$) are found and confirmed by several numerical schemes.
- Eight-band model is required to describe such a Dirac point and the split Weyl points. More interesting yet complicated behaviors are expected in ternary (and beyond) 194-materials .